10th International IFAC Symposium on
Computer Applications in Biotechnology
Preprints Vol.1, June 4-6, 2007, Cancún, Mexico

SIMPLE 3D VASCULARIZATION MODELS FOR PERFUSION BIOREACTORS

Francesco Coletti and Sandro Macchietto[1]

Department of Chemical Engineering, Imperial College London
South Kensington campus, London SW7 2AZ, UK

Abstract: Growing cells in a perfusion bioreactor for tissue engineering is challenging. Cell viability and distribution is determined by complex interactions between a medium flowing through a porous scaffold and cell growth. Using a mathematical model that includes oxygen transport by diffusion/convection and cell growth mechanism, the effect of simple vascularization within the scaffold is investigated. As an initial approximation, straight channels through the length of the scaffold are considered, with performance assessed using a systematic set of criteria. Results indicate the approach can inform the choice of suitable channel size and spacing, and should enable enhanced scaffold design.

Keywords: Perfusion bioreactors, biomedical systems, mathematical models, dynamic models, performance analysis.

1. INTRODUCTION

Growing *in vitro* graft for tissue engineering presents many challenges. Achieving a uniform oxygen distribution as well as a high cell density within a three-dimensional (3D) scaffold is one of the major issues (Lewis *et al.,* 2005; Obradovic *et al.,* 2000; Radisic *et al.,* 2006). In recent years, perfusion bioreactors have been successfully used to overcome problems related to oxygen delivery (Bancroft *et al.,* 2003; Glowacki *et al.,* 1998; Goldstein *et al.,* 2001) and these are the subject of this study. Problems remain in growing tissues of clinical relevant thickness and further advances are required.

1.1 The vascularization approach.

In vivo tissues receive the necessary substrate for proliferation from the circulatory system through capillaries. Mimicking the natural tissue vascularization can lead to the formation of more homogeneous tissues and prevents implant failure caused by hypoxia (Markowicz *et al.,* 2005). Unfortunately, the production of an intricate network of capillaries within a polymeric scaffold is difficult to achieve. It has been demonstrated that low oxygen partial pressure outside the cells (Semenza 2001) can induce vasculogenesis (new blood vessel formation) and angiogenesis (formation of new branches of pre–existing vessels). Some experimental work was done on vascularization *in vitro* (Kirkpatrick *et al.,* 2003; Levenberg *et al.,* 2005), but hardly any paper considers this issue from a modelling point of view, as an aid to provide an understanding of the fundamental mechanisms regulating oxygen flow to a scaffold. Pettet *et al.* (1996) correlate density of vessels to oxygenated areas for a wound–healing process, but results seems difficult to adapt to a scaffold–bioreactor system. Ma *et al.* (2005) modelled the effects of structure on the nutrient distribution for *in vivo* bone marrow, however, for an RWPV bioreactor as opposed to the total perfusion type considered here. For perfusion bioreactors, Radisic *et al.* (2004) model oxygen distribution in a scaffold with a parallel channel array as a mimic to real tissue vascularization, but assume constant cell density and the model, therefore, is in steady–state. A major limitation is that velocities in the porous matrix are neglected so that only diffusion and

[1] Corresponding author: Prof. Sandro Macchietto
Department of Chemical Engineering
Imperial College London, South Kensington campus
London SW7 2AZ, UK
tel. +44 (0)207 594 6608
email: s.macchietto@imperial.ac.uk

reaction but not perfusion are accounted for in the tissue space.

A systematic modelling study of the effects of channel structure in a scaffold in perfusion bioreactors, aimed at understanding the evolution of cell density and distribution, appears to be lacking.

2. METHODS AND OBJECTIVES

The long term goal is to develop a fundamental understanding of vascularization on oxygen transport and cell growth within a perfusion bioreactor. A mathematical model already developed (Coletti *et al.,* 2006) is used which describes a 3D cell culture in cylindrical perfusion bioreactors, including the complex interactions between fluid dynamics of a nutrient medium flowing by convection and diffusion through a scaffold, modelled as a porous medium, and cells growth kinetics. Here, the model is adapted to include a simple vascularization, in the form of straight channels through the scaffold.

First the effect of a single, straight channel at the centre of the scaffold is analysed in 2D, exploiting the symmetry of this geometry with respect to the angular coordinate. A more complex, 3D geometry with several channels is then considered, with the assumption of angular symmetry relaxed. Results are compared to a reference base case with full perfusion (no channels) under the same operating conditions (medium flowrate and composition, cell type, etc.). The parameters used are for immortalised murine C_2C_{12} cell culture on a collagen scaffold.

The aims are to keep the oxygen concentration in the scaffold above a viability level below which the culture enters critical conditions (hypoxia), and to achieve a high and homogeneous final cell distribution as fast as possible. To properly evaluate alternative configurations and operations, some systematic criteria are needed and these are described first.

2.1 Performance assessment criteria.

Changing operating conditions, reactor or scaffold geometry, or cell line parameters affect cells growth in a very complex way. Oxygen and cell concentration are a function of local conditions and evolve in time, and in a 3D scaffold are therefore functions of (z,r, ϑ ,t). Aggregate criteria are however useful to compare overall conditions at any one time, and their evolution in time. A set of 7 systematic criteria by which to evaluate the performance of alternative operations proposed by Coletti and Macchietto (2006) is briefly summarized here, with performance defined in terms of oxygen concentration and uniformity of its distribution within the scaffold. Some of the criteria may be applied to other relevant quantities of interest, such as cell density or oxygen uptake rate.

Criterion A1. $\overline{c}_{O_2}$, at time *t*, the oxygen average concentration in the scaffold:

$$\overline{c}_{O_2} = \frac{\int_{V_s} c_{O_2}(r,z,\vartheta,t)\, dV_s}{V_s} \tag{1}$$

where V_s is the scaffold total volume, r, z and ϑ are the systems coordinate and c_{O2} is the local oxygen concentration in the scaffold.

Criterion A2. $\overline{c}^{\%}_{O_2}$, at time *t*, $\overline{c}_{O_2}$ as a percent of the limit oxygen concentration for viability, c_{lim}:

$$\overline{c}^{\%}_{O_2} = \frac{\overline{c}_{O_2}}{c_{\lim}} \cdot 100 \tag{2}$$

Criterion B. $\tilde{t}_B$: the time when $\overline{c}_{O_2}$ first falls below c_{lim}:

$$\tilde{t}_B = t\big|_{\overline{c}_{O_2} < c_{\lim}} \tag{3}$$

Criterion C. The location ($\tilde{r}$, $\tilde{z}$, $\overline{\vartheta}$) and time $\tilde{t}_C$ where the oxygen concentration first falls below the viability level, $c_{lim:}$

$$\begin{cases} \tilde{r}_C, \tilde{z}_C, \overline{\vartheta}_C = (r,z,\vartheta)\big|_{\overline{c}_{O_2} < c_{\lim}} \\ \tilde{t}_C = t\big|_{\overline{c}_{O_2} < c_{\lim}} \end{cases} \tag{4}$$

Criterion D. $\tilde{V}_D$, at time *t*, the fraction of scaffold volume (in percent) with $c_{O2} < c_{lim:}$

$$\tilde{V}_D = \frac{\int_{V_s} V\big|_{\overline{c}_{O_2} < c_{\lim}}\, dV_s}{V_s} \cdot 100 \tag{5}$$

Criterion E. $\tilde{t}_E^{\,p\%}$, the time when a given percentage volume *p*% of the scaffold has $c_{O2} < c_{lim}$:

$$\tilde{t}_E^{\,p\%} = t\big|_{\tilde{V}_D < p} \tag{6}$$

Criterion F1. A_{O_2} , at time *t*, the amount of oxygen available for cells metabolism in the scaffold:

$$A_{O_2} = \int_0^{\mathrm{R}} \int_0^{2\pi} N_{O_2}\big|_{z^{out}} - N_{O_2}\big|_{z^{in}}\, d\vartheta dr \tag{7}$$

where N_{O_2} is the oxygen total flux into (Z^{in}) and out (Z^{out}) of the scaffold.

Criterion F2. $A^{\%}_{O_2}$, at time *t*, the amount of oxygen used by the cells as a % of the total oxygen inlet:

$$A^{\%}_{O_2} = \frac{A_{O_2}}{\int_0^{\mathrm{R}} \int_0^{2\pi} N_{O_2}\big|_{z^{in}}\, d\vartheta dr} \tag{8}$$

Criterion G. At time *t*, oxygen distribution, as a histogram where each bar is the fraction of scaffold volume that has oxygen concentration between two

defined levels. A high fraction of scaffold volume within a few adjacent concentration bars indicates a uniform distribution.

3. SIMULATIONS AND RESULTS

3.1 Single channel effects.

A cylindrical perfusion reactor is considered with reference geometry given in Fig. 1 (with angular symmetry around the z axis). The oxygenated medium flows upwards at constant overall rate determined by a peristaltic pump. Coletti *et al.* (2006) give assumptions, model equations, boundary conditions, parameters for typical cell types and results for the cases of full perfusion (no channels) and some channelling at the wall. The analysis shows that as cells grow and occupy larger portions of the scaffold void (mainly in the bottom layers of the scaffold where oxygenation is greater), the resistance to perfusion increases, larger amounts of oxygen are taken up by cells in the bottom layers, and cells in the upper layers do not grow (or die).

Here, a single straight channel at the centre of the scaffold is first simulated to asses the effect of channel size on transport and growth inside the bioreactor. The channel allows some fresh medium (with c_{O_2} at the saturation level) to reach the upper sections of the scaffold. Oxygen can diffuse from the channel lateral wall (at distance δ from the centre of the bioreactor) into the scaffold in the radial direction. On the other hand, the channel provides a shot-cut path for the medium flow, decreasing the convective oxygen transport through the porous scaffold matrix. The relative importance of the two effects on cell growth (positive, due to the extra diffusion to the upper layers and negative, due to flow bypass) depends on the channel size and (time varying) scaffold porosity. It is therefore important to establish whether the overall effect is positive or not. Due to symmetry, simulations are required only on one half of the 2D system. All calculations were performed using COMSOL Multiphysics (COMSOL, Stockholm, Sweden) with suitable grids and numerical methods. For the Base Case conditions given in Coletti *et al.* (2006), Fig. 2 shows an arrow plot of the diffusive (a) and convective (b) oxygen flux after 7 days of culture. The channel radius $\delta = 10^{-4}$ m is an order of magnitude larger than the average pore radius of the scaffold (a collagen

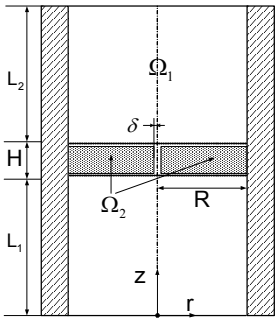

Fig. 1. Reference geometry and system co–ordinates.

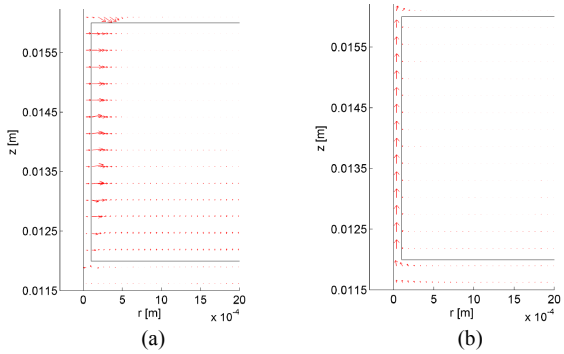

Fig. 2. Arrow plot of diffusive (a) and convective(b) flux. Singe central channel radius $\delta = 10^{-4}$ m.

sponge with an initial porosity of 97%). The diffusive flux in the downstream sections of the scaffold is perpendicular to the axis of the channel whereas the convective flux is parallel to it. Fig. 3 shows the diffusive (a) and the convective (b) fluxes after 6 days of culture over a section that starts at the channel lateral wall at z=0.015 and extends in the radial direction for 1 mm in the case of diffusive flux and 0.5 mm in case of convective flux. The diffusive flux is two orders of magnitude smaller than the convective one. The former extends to higher r–coordinates (up to ~8 times the channel radius) than the latter. The convective flux vanishes after approximately 0.5 mm from the channel lateral wall (i.e. ~5 times the channel radius).

Channel size effect. The channel radius affects the distance from the channel's lateral wall where the oxygen concentration is kept above the viability level. Fig. 4 shows the limit concentration front after 6 days of culture in the scaffold, for channels of radius $\delta = 10^{-5}$ m (a) and $\delta = 10^{-4}$ (b). Below the front the oxygen concentration is above the viability limit, c_{lim}. Fig. 4.b shows that the channel raises the oxygen concentration in some deeper sections of the scaffold (even if only for a small distance from the channel

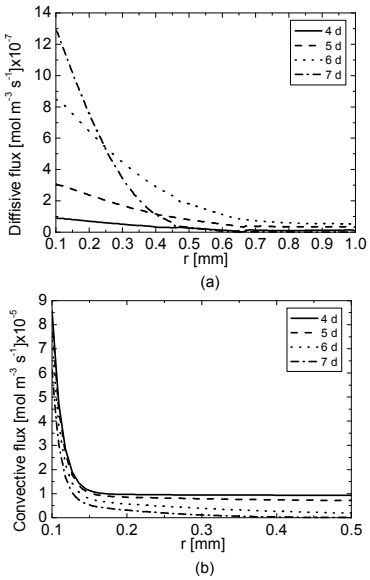

Fig. 3. Diffusive (a) and convective (b) flux on a section taken at z=0.015 m., starting from the channel lateral wall, for channel radius $\delta = 10^{-4}$ m.

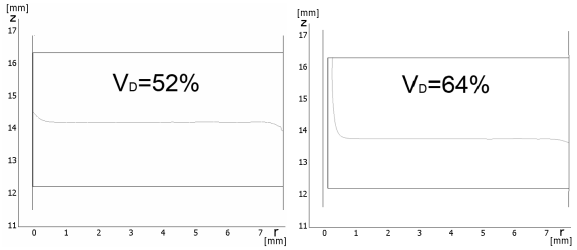

(a) (b)

Fig. 4. Limit oxygen concentration front and fraction of scaffold above the viability level (V_D) after 6 days of culture. Channel radius $\delta = 10^{-5}$ m, (a) and $\delta = 10^{-4}$ m, (b). In case (a) the channel is not clearly visible because of the scale of the picture.

lateral edge) that were otherwise below the viability level. Fig. 4a gives the corresponding profile with a channel radius of 10^{-5} m (very small, close to average pore size). It shows that a smaller channel contributes to a smaller raise in oxygen concentration in the r–direction, away from the channel lateral wall. Distinct transport phenomena dominate in the two cases. With a larger channel, the diffusive flux is higher in the zones close to the channel wall whereas the convective flux inside the scaffold is lower. Due to flow bypass and decreased perfusion through the matrix, the fraction of scaffold below the viability level, V_D, is greater with the larger channel (Fig. 4b) than with the smaller one (Fig. 4a).

3.2 Multiple channels.

In order to consider more complex vascularization geometries the symmetry assumptions leading to a 2D simulation must be relaxed. A 3D geometry with multiple straight channels is analysed in this section.

Reference system. To avoid simulating the entire bioreactor volume, a 20 degree "wedge" with a single channel (Fig. 5, shown horizontally for clarity) is actually simulated, taking advantage of angular symmetry. This wedge has its vertex on the central axis of the bioreactor, a width equal to the bioreactor radius R, and extends for the whole length of the bioreactor. This volume represents the behaviour of the entire bioreactor if the section is considered as a unit repeating 18 times (360/20 degrees). Symmetry is imposed on the lateral faces of the chosen wedge

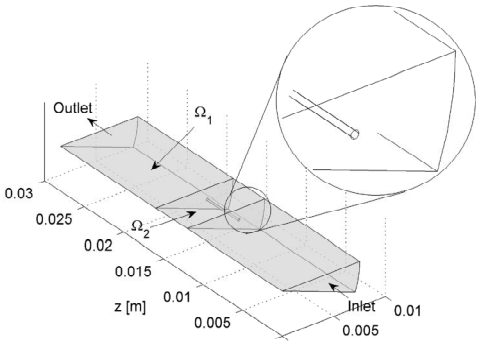

Fig. 5. Bioreactor geometry with channelled scaffold. The channel has its centre (Cartesian coordinates, in m) at (0.005,0.016,-0.001).

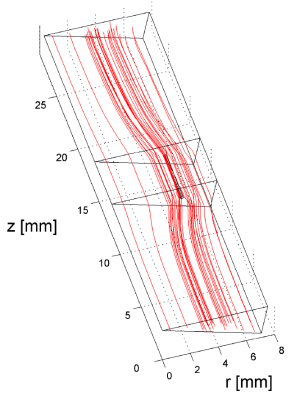

Fig. 6. Velocity streamlines in the bioreactor. The channel deviates the flux of the medium.

and along the vertex, which represents the centre of the entire bioreactor, by means of suitable boundary conditions. The channel ($\delta = 10^{-4}$) is placed arbitrarily approximately in the middle of this 3D section.

Fluid dynamics. As noted, the presence of a channel provides a path of lower resistance to the fluid flow than the porous scaffold matrix. To show the effect of the channel on flow re-distribution between channel and matrix, the streamline of the velocities in domains Ω_1 (entrance section), Ω_2 (scaffold) and Ω_3 (exit section) are plotted in Fig. 6. Quantitatively, the channel effect can be evaluated as the ratio of medium flow through the channel to that through the scaffold (not only from the entry surface ($z = z^{in}$) but also through the channel lateral surface). The volumetric flow into the scaffold from its bottom surface (z=0.012 here) is the integral of the velocity field on that surface:

$$\dot{V}_S^{in} = \int_{A_S} \mathbf{v} dA_S \qquad (9)$$

where A_S is the cross–sectional area of the scaffold domain (scaffold total cross–sectional area minus the cross–sectional area of the channel). The flow of medium entering the open channel, $\dot{V}_C^{in}$, is calculated as the difference between the bioreactor's overall inlet flow $\dot{V}$ and the flow trough the scaffold, $\dot{V}_S^{in}$. Moreover, the growth of the cells itself increases the resistance to medium flow due to the decrease in void space in the scaffold over time. This produces a drop in the porosity of the matrix and an increase in

Table 1 Flow through the scaffold bottom surface, through the channel and ratio of the latter to the total flow into the bioreactor (in %).

Time[d]	$\dot{V}_S^{in}$ [m^3 s^{-1}]	$\dot{V}_C^{in}$ [m^3 s^{-1}]	$\dot{V}_C^{in}/\dot{V}$ [%]
0	8.87×10^{-10}	3.91×10^{-11}	4.22
1	8.87×10^{-10}	3.91×10^{-11}	4.22
2	8.87×10^{-10}	3.91×10^{-11}	4.22
3	8.87×10^{-10}	3.91×10^{-11}	4.22
4	8.87×10^{-10}	3.92×10^{-11}	4.24
5	8.86×10^{-10}	3.96×10^{-11}	4.28
6	8.85×10^{-10}	4.08×10^{-11}	4.41
7	8.83×10^{-10}	4.31×10^{-11}	4.65

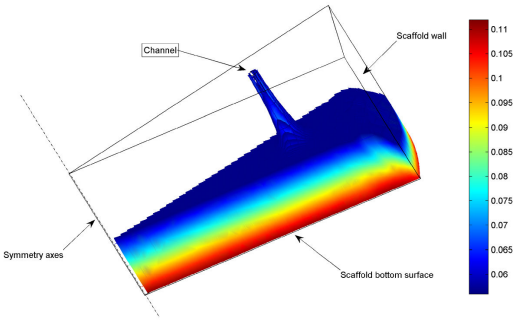

Fig. 7. Oxygen concentration in the scaffold (range between the viability and the saturation levels). The volume in white is below the viability level.

its tortuosity, which affect the channel/scaffold flow ratio. For the case considered, after 7 days of culture, the flowrate into the channel is 4.3073×10^{-11} m^3 s^{-1} (=0.0437 mm^3 s^{-1}) that is 4.65% of the total flowrate into the bioreactor. This is very high considering that the channel has a cross–sectional area A_C = 3.1415×10^{-8} m^2, only 0.32% of the overall bioreactor section. Table 1 reports the flowrates through the channel and the ratios of flows $\dot{V}_C^{in}/\dot{V}$ at different times of culture. Initially, the flow distribution is not influenced by the growth of the cells. After day 4, the flow through the channel is slightly increased as the higher cell density produces a decrease in the permeability large enough to impede the flow through the porous matrix, but this effect is not very large.

3.3 Analysis of scaffold performance.

A 3D view highlighting the volume where oxygen is above the viability level is shown in Fig 7, with colours representing an oxygen concentration range in the scaffold between the viability and the saturation levels. The portion of scaffold volume with oxygen below the viability limit is indicated in white. The sectional view clearly highlights the influence of the channel in supplying oxygen to the

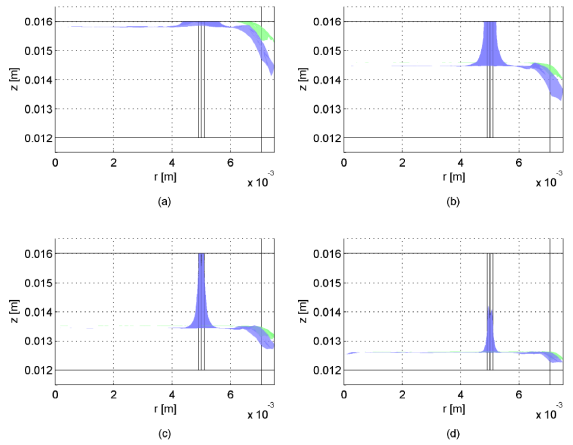

Fig. 8. Limit concentration (0.056 mol m^{-3}) for Base Case (green) and channelled case 3.2 (blue) at day 5 (a), day 5.5 (b), day 6 (c) and day 7(d). Boundary effects of the scaffold wall on the profiles are also noted.

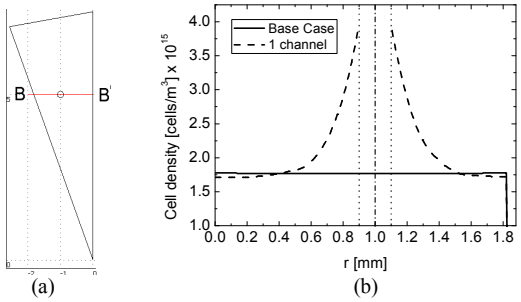

Fig. 9. Section fixed by a line that passes through the diameter of the channel and is perpendicular to the to the plane ϑ=0. The cell density profiles are shown in (b). The vertical dashed lines indicate the channel's lateral walls and the dash-dot line its centre.

areas in its immediate vicinity. This is seen by the darker colours around the channel, through the entire scaffold depth. The channel, which brings fresh medium to greater depths within the porous structure, feeds oxygen to the areas around it, mostly by diffusion and partly by convection, keeping them above the viability level. This suggests that cell growth is possible in a zone around the channel for the entire depth of the scaffold.

Comparison with the Base Case. In the reference Base Case the bioreactor runs under the same operating conditions at full perfusion (no channels). Fig. 8 shows the oxygen viability level over 3 days for the Base Case and the channelled 3D case of section 3.2. In the former, the viability level profile is flat along the scaffold radius and a slightly larger fraction of the scaffold volume is viable, compared to the latter. In the channelled case, a volume around the channel for a distance up to about 4 times the channel radius (Fig. 8.a and 8.b) is kept above the viability level of 0.056 mol m^{-3} until day 6 of culture. This effect is much lower at day 7 (Fig. 8.d). To illustrate the channel effect on cell density, the cell density distribution along section (BB' in Fig. 9a, through the channel diameter and perpendicular to the plane ϑ=0), is shown in Fig 9.b. The cell density near the channel (up to ~2 times its radius) is up to about twice the value of the cell density in the rest of the scaffold.

Performance evaluation. So far, a detailed analysis was presented of the dynamic behaviour of cells and oxygen concentration in the bioreactor. However, it

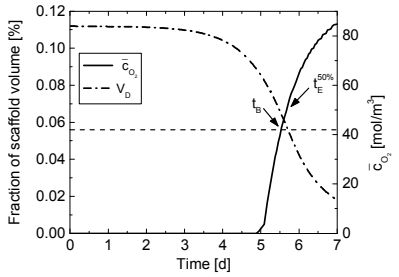

Fig. 10. Criteria A, B, D and E applied to the single channel case in three dimensions.

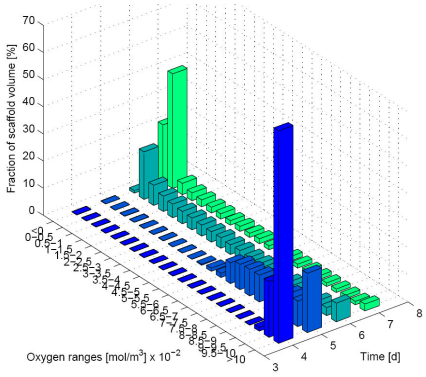

Fig. 11. Oxygen distribution in channelled scaffold.

is still not evident whether an overall beneficial effect is given by the channel. This assessment can be done through the systematic analysis proposed by Coletti and Macchietto (2006). Fig. 10 reports numerical values for some of their criteria for case 3.2. The average oxygen concentration falls below the viability level at $\tilde{t}_B$ =5.71 days and half of the scaffold ($\tilde{V}_D^{50\%}$) is below the viability level after 5.67 days. These data are slightly poorer than the equivalent for the base case. Fig. 11 shows the oxygen concentration distributions between days 3 and 7 of culture. The overall distribution is only marginally worse than in the base case. With only one channel per "wedge", the positive local effects are limited to the small volume around it, and mildly offset by the oxygen bypass though the channel.

5. CONCLUSION

Using a model that couples flow and cell growth dynamics, this study highlighted quantitatively the trade-off between convective flux in the porous matrix and diffusion from the channel lateral surface. The extension of the model to a 3D geometry made it possible to investigate the effects of a single channel in an arbitrary position inside a 20 degrees slice of the bioreactor. Channels in the scaffold matrix are found to provide significant local benefits in terms of supplying oxygen to parts that are otherwise difficult to reach. Large channels however allow the medium to partially bypass the scaffold decreasing the convection contribution to oxygen transfer. On the other hand, channels with radius of the order of the pores size provide negligible diffusional benefits. Clearly there is an interesting optimisation problem here. A quantitative comparison of alternative configurations was enabled by the use of systematic performance assessment criteria. The methods presented should make it possible to analyse, and eventually design, suitable 3D vascularization structures for tissue engineering in bioreactors.

REFERENCES

Bancroft, G. N., V. I. Sikavitsas and A. G. Mikos (2003). Design of a flow perfusion bioreactor system for bone tissue-engineering applications. *Tissue Engineering* **9**(3): 549-554.

Coletti F, S. Macchietto, N. Elvassore (2006). Mathematical modeling of three-dimensional cell cultures in perfusion bioreactors. *Industrial & Engineering Chemistry research* **45**(24):8158-8169.

Coletti, F. and S. Macchietto (2006). Evaluating and improving performance in perfusion bioreactors – A modelling study. *Submitted*.

Glowacki, J., S. Mizuno and J. S. Greenberger (1998). Perfusion enhances functions of bone marrow stromal cells in three-dimensional culture. *Cell Transplantation* **7**(3): 319-326.

Goldstein, A. S., T. M. Juarez, C. D. Helmke, M. C. Gustin and A. G. Mikos (2001). Effect of convection on osteoblastic cell growth and function in biodegradable polymer foam scaffolds. *Biomaterials* **22**(11): 1279-1288.

Kirkpatrick, C. J., R. E. Unger, V. Krump-Konvalinkova, K. Peters, H. Schmidt and G. Kamp (2003). Experimental approaches to study vascularization in tissue engineering and biomaterial applications. *Journal of Materials Science: Materials in Medicine* **V14**(8): 677-681.

Levenberg, S., P. A. D'Amore, C. A. Van Blitterswijk, E. S. Garfein, R. C. Mulligan*, et al.* (2005). Engineering vascularized skeletal muscle tissue. *Nature biotechnology* **23**(7): 879-884.

Lewis, M. C., B. D. MacArthur, J. Malda, G. Pettet and C. P. Please (2005). Heterogeneous proliferation within engineered cartilaginous tissue: the role of oxygen tension. *Biotechnology and Bioengineering* **91**(5): 607-615.

Ma, C. Y. J., A. Mantalaris and X. Y. Xu (2005). *Development of a Mathematical Model for a 3-D Perfused Bone Marrow Culture System*. Aiche annual meeting 2005.

Markowicz, M., E. Koellensperger, S. Neuss, G. C. Steffens and N. Pallua (2005). *Topics in Tissue Engineering, Enhancing the Vascularization of Three-Dimensional Scaffolds*, N. Ashammakhi & R.L. Reis.

Obradovic, B., J. H. Meldon, L. E. Freed and G. Vunjak-Novakovic (2000). Glycosaminoglycan deposition in engineered cartilage: Experiments and mathematical model. *AIChE Journal* **46**(9): 1860-1871.

Pettet, G. J., H. M. Byrne, D. L. McElwain and J. Norbury (1996). A model of wound-healing angiogenesis in soft tissue. *Mathematical Bioscience* **136**(1): 35-63.

Radisic, M., J. Malda, E. Epping, W. Geng, R. Langer and G. Vunjak-Novakovic (2006). Oxygen gradients correlate with cell density and cell viability in engineered cardiac tissue. *Biotechnology and Bioengineering* **93**(2): 332-343.

Radisic, M., L. Yang, J. Boublik, R. J. Cohen, R. Langer, L. E. Freed and G. Vunjak-Novakovic (2004). Medium perfusion enables engineering of compact and contractile cardiac tissue. *Am J Physiol Heart Circ Physiol* **286**(2): H507-516.

Semenza, G. L. (2001). Regulation of hypoxia-induced angiogenesis: a chaperone escorts VEGF to the dance. *J. Clin. Invest.* **108**(1): 39-40.